An Algorithm for Solving Torsional Vibration Problems Based on the Invariant Imbedding Method

Antonio Lopes Gama

Department of Mechanical Engineering, Universidade Federal Fluminense-UFF, 24210-000, Niterói, RJ, Brazil.

Rafael Soares de Oliveira

National Institute of Metrology-INMETRO, 25250-020, Duque de Caxias, RJ, Brazil.

(Received 25 September 2012; provisionally accepted 20 August 2013; accepted 18 September 2013)

In this work the invariant imbedding method has been used to develop an algorithm to study the torsional vibration of non-uniform systems. The algorithm is based on the propagation, reflection, and transmission of waves in a stepped waveguide and is part of a procedure to transform two-point boundary value problems in initial value problems. Based on this approach, a continuous model has been developed and a simple, versatile, and robust algorithm has been constructed to solve torsional vibration problems of non-uniform shafts with circular cross-sections. The proposed solution algorithm was extensively evaluated through comparisons with analytical solutions and the finite element method. The results show that the proposed method can provide the exact solution for uniform shafts with concentrated elements and accurate results for a wide variety of torsional vibration problems. Systems with continuously varying geometry may be approximated by stepped shafts. The proposed method can also be used to study the dynamic behaviour of others stepped systems.

1. INTRODUCTION

In the present paper, an approach usually applied to investigate the wave propagation in layered media is used to develop a continuous model to study the torsional vibration of non-uniform systems.[1] The formulation of the proposed method considers that partial torsional waves propagate in opposite directions in a system with stepped changes in its properties as shown in Fig. 1. In the frequency domain, the governing equations are written in a state space form where the state variables are the angular displacement and twisting moment. The state matrix varies in a piece-wise constant fashion according to the properties of each segment of the rod. The part of the rod with continuously varying geometry (e.g., a conical part) is approximated by thin uniform segments. The solution of the state space equation is obtained by employing a discrete version of the Riccati transformation, which is a key ingredient in the invariant imbedding approach.[2] This technique is used to transform two-point boundary value problems in initial value problems, and is also known as the method of sweeps, the Riccati method, or the factorization method.[3,4] Based on this transformation, a recursive algorithm has been constructed for the solution, providing a simple and powerful computational method capable of solving problems of torsional vibration in circular non-uniform rods.[5,6] Comparisons to analytical solutions and finite element results show that the proposed method can provide the exact solution for the torsional vibration of uniform shafts with concentrated elements and an approximated solution for shafts with a continuously varying geometry.

It must be pointed out that previous works have considered the propagation, reflection, and transmission of waves to solve vibration problems in finite inhomogeneous systems.[7,8] It must also be mentioned that other methods to obtain the solution for the torsional vibration of non-uniform rods have been presented in the literature. An analytical solution was provided by Pouyet and Lataillade[9] for specific profiles of non-uniform rods, and the exact solution for more general cases has been obtained by Qiao et al.[10] and Li.[11] A continuous model for stepped shafts was proposed by Mioduchowski,[12] and a general approach for stepped systems governed by the one-dimensional wave equation was presented by Bapat and Bhutani.[13] A new exact approach for the analysis of torsional vibration of a non-uniform shaft carrying an arbitrary number of rigid disks has been proposed by Chen.[14] Xiang et al.[15] used the modified Riccati torsional transfer matrix method to calculate the torsional natural frequencies of a shaft system modelled as a chain consisting of an elastic spring with concentrated mass points.

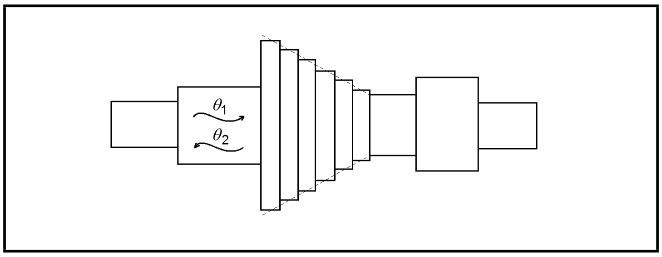

Figure 1. Stepped shaft with a conical part approximated by cylindrical segments.

As described in the foregoing sections, the main contribution of the present work is to provide a simple and concise algorithm that is able to solve a great variety of vibration problems. The algorithm can be easily implemented and used to solve the forced torsional vibration of non-uniform systems with classical or non-classical boundary conditions. Although the proposed method has been developed to study the vibration of systems governed by the one-dimensional wave equation, the algorithm presented here can also be applied to study the dynamic behaviour of other stepped systems. In fact, this method has been used by the author to investigate the high frequency response of stepped layered composite beams, where the discrete form of the Riccati transformation has been used to solve a stiff system of ordinary differential equations.[6]

2. THE STATE SPACE EQUATION

The algorithm presented in this work to study the vibration of stepped systems will be used for solving the torsional vibration of non-uniform rods. In the proposed method, the rod is treated as one formed by a series of cylindrical segments. The state space equation is formulated assuming that each cylindrical part is elastic, homogeneous, and isotropic. It is also considered that the angular motion occurs as a rotation of the cross-sectional area as a whole; i.e., all the points of a cross-section present the same angular displacement.

From mechanics of solids, the relationship between the angular displacement $\overline{\theta}(x,t)$ and the twisting moment $\overline{M}(x,t)$ is given by:

$$\frac{\partial\overline{\theta}(x,t)}{\partial x} = \frac{\overline{M}(x,t)}{GJ(x)}; \tag{1}$$

where G is the shear modulus of elasticity and J is the polar area moment of inertia of the shaft cross-section. The equation of motion for the free torsional vibration is written as

$$\frac{\partial\overline{M}(x,t)}{\partial x} = I(x)\frac{\partial^2\overline{\theta}(x,t)}{\partial t^2}; \tag{2}$$

where $I(x)$ is the polar mass moment of inertia per unit length. If the time dependence of $\overline{\theta}(x,t)$ and $\overline{M}(x,t)$ is harmonic and represented by functions of the form $\overline{\theta}(x,t) = \theta(x)e^{-i\omega t}$ and $\overline{M}(x,t) = M(x)e^{-i\omega t}$, Eqs. (1) and (2) reduce to:

$$\frac{d\theta(x)}{dx} = \frac{M(x)}{GJ(x)}; \tag{3a}$$

$$\frac{dM(x)}{dx} = -\omega^2 I(x)\theta(x). \tag{3b}$$

Using Eqs. (3a) and (3b), a state space equation is written in a matrix form as

$$\frac{d\boldsymbol{\zeta}}{dx} = \mathbf{T}\boldsymbol{\zeta}; \tag{4}$$

where $\boldsymbol{\zeta}$ is the state vector and $\mathbf{T}$ is the state matrix given by:

$$\boldsymbol{\zeta} = \begin{Bmatrix} \theta(x) \\ M(x) \end{Bmatrix}; \tag{5a}$$

$$\mathbf{T} = \begin{bmatrix} 0 & \frac{1}{GJ} \\ -\omega^2 I & 0 \end{bmatrix}. \tag{5b}$$

3. SOLUTION OF THE STATE SPACE EQUATION

The solution of the state space equation is based on the invariant imbedding method where a two-point boundary value problem is transformed in an initial value problem.[1–4] The purpose of the following procedure is to find a solution for Eq. (4) in the form

$$M(x) = K(x)\theta(x); \tag{6}$$

where $K(x)$ is called here the global torsional stiffness. Of course, in general $K(x)$ depends on the material and geometry of the rod, as well as frequency.

The solution of Eq. (4) may be written as

$$\boldsymbol{\zeta}(x) = \mathbf{N}(x)\boldsymbol{\zeta}(0); \tag{7}$$

where $\mathbf{N}$ is the transfer matrix that relates the state vector in a position x to its value in the initial position $x = 0$, and has the form

$$\mathbf{N}(x) = e^{\mathbf{T}x}. \tag{8}$$

Writing the matrix $\mathbf{T}$ in function of their eigenvalues and eigenvectors, one can rewrite Eq. (8) as

$$\mathbf{N}(x) = \mathbf{V}\left\{\mathrm{diag}[e^{k_1 x}, e^{k_2 x}]\right\}\mathbf{V}^{-1}; \tag{9}$$

where $\mathbf{V}$ is the matrix whose columns are the eigenvectors, and k_α, $\alpha = 1, 2$, are the eigenvalues of the state matrix $\mathbf{T}$. The eigenvalues of $\mathbf{T}$ are the wave numbers of partial waves that propagate in the positive and negative direction of the x-axis and are related as $k_2 = -k_1$. Separating the eigenvalues and eigenvectors according to waves that propagate in the positive and negative direction of the x-axis, the matrix $\mathbf{v}$ is decomposed as

$$\mathbf{V} = \begin{bmatrix} A_1 & A_2 \\ L_1 & L_2 \end{bmatrix}; \tag{10}$$

where A_α and L_α, $\alpha = 1, 2$, are components of the eigenvectors of $\mathbf{T}$. The subscripts 1 and 2 are associated to the waves that propagate in the positive and negative direction of the x-axis, respectively.

The state vector in the initial position $x = 0$ may be expressed as a linear combination of the eigenvectors of matrix $\mathbf{T}$ as

$$\boldsymbol{\zeta}(0) = \mathbf{V}\mathbf{c} = \begin{bmatrix} A_1 & A_2 \\ L_1 & L_2 \end{bmatrix}\begin{Bmatrix} c_1 \\ c_2 \end{Bmatrix}; \tag{11}$$

where $\mathbf{c}$ is a constant vector. Substituting Eqs. (9) and (11) into Eq. (7) yields

$$\boldsymbol{\zeta}(x) = \begin{bmatrix} A_1 & A_2 \\ L_1 & L_2 \end{bmatrix}\begin{bmatrix} W_1(x) & 0 \\ 0 & W_2(x) \end{bmatrix}\begin{Bmatrix} c_1 \\ c_2 \end{Bmatrix}; \tag{12}$$

where $W_1(x) = W_2^{-1}(x) = e^{k_1 x}$ are called here the propagator functions. At this point, the state variables $\theta(x)$ and $M(x)$ will be separated in two parts, corresponding to the contributions to the total fields of the partial waves that propagate in opposite directions. This is a common practice in the description of wave motion in layered media and is an important feature of the method of solution presented in this work.[5] As mentioned before, the subscripts 1 and 2 are related respectively to the waves that propagate in the positive and negative direction of the x-axis. The angular displacement $\theta(x)$ and the twisting moment $M(x)$ are now represented as a result of waves that propagate in the positive and negative direction of the x-axis as

$$\theta(x) = \theta_1(x) + \theta_2(x) \tag{13a}$$

and

$$M(x) = M_1(x) + M_2(x). \tag{13b}$$

According to Eq. (12), each component of the variables $\theta(x)$ and $M(x)$ in Eqs. (13a) and (13b) are given by

$$\theta_\alpha(x) = A_\alpha W_\alpha(x) c_\alpha \tag{14a}$$

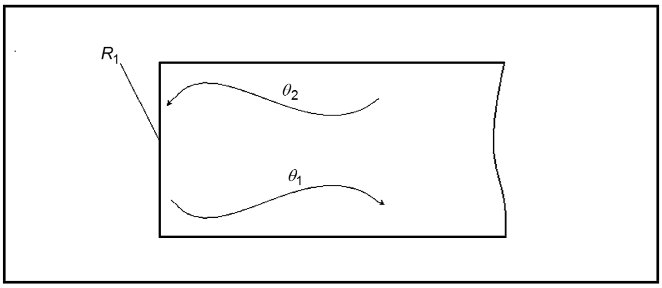

Figure 2. Partial waves propagating in a rod.

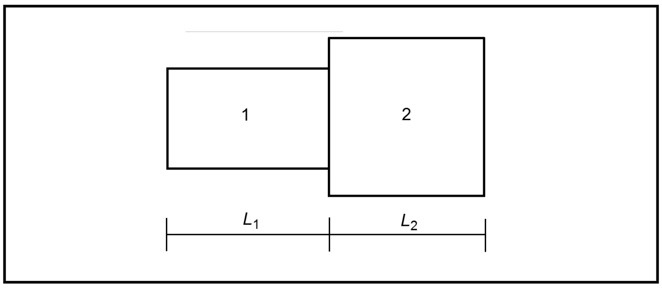

Figure 3. Rod composed of two uniform segments.

and

$$M_\alpha(x) = L_\alpha W_\alpha(x) c_\alpha; \tag{14b}$$

where $\alpha = 1, 2$. The constants $c_\alpha = \theta_\alpha(0)/A_\alpha$ are determined from Eq. (14a) at $x = 0$; therefore, Eqs. (14a) and (14b) are rewritten as

$$\theta_\alpha(x) = W_\alpha(x)\theta_\alpha(0) \tag{15a}$$

and

$$M_\alpha(x) = L_\alpha W_\alpha(x)\frac{\theta_\alpha(0)}{A_\alpha}. \tag{15b}$$

The propagator functions $W_\alpha(x)$ relate the positive ($\alpha = 1$) and negative ($\alpha = 2$) partial waves with its value at $x = 0$. From Eq. (15a), $\theta_\alpha(0)$ is obtained and substituted in Eq. (15b) as

$$M_\alpha(x) = S_\alpha \theta_\alpha(x); \tag{16}$$

where $S_\alpha = \frac{L_\alpha}{A_\alpha}$ is called here the local torsional stiffness of the rod. It must be pointed out that both $W_\alpha(x)$ and S_α are functions of the geometry and material properties of each uniform part of the rod and of the pair (k, ω). Substitution of Eq. (16) in Eq. (13b) results in

$$M(x) = S_1\theta_1(x) + S_2\theta_2(x). \tag{17}$$

Consider now a torsional wave $\theta_2(x)$ propagating in the negative direction of the x-axis, next impinging on the left end of the rod ($x = 0$), and being reflected as a wave $\theta_1(x)$ propagating in the positive direction of the x-axis, as shown in Fig. 2. At $x = 0$, these waves are related by the reflection coefficient R_1 (Fig. 2):

$$\theta_1(0) = R_1\theta_2(0). \tag{18}$$

From the relationship between the partial waves given by Eq. (15a) and Eq. (18), Eq. (13a) may be written as

$$\theta(x) = [H(x) + 1]\theta_2(x); \tag{19}$$

where

$$H(x) = \frac{W_1(x)R_1}{W_2(x)}. \tag{20}$$

Using Eqs. (19) and (20), Eq. (17) becomes

$$M(x) = S_1H(x)\theta_2(x) + S_2\theta_2(x). \tag{21}$$

Finally, obtaining $\theta_2(x)$ from Eq. (19) and substituting in Eq. (21) one has the expression relating the twisting moment and the angular displacement in the desired form of Eq. (6) as

$$M(x) = \frac{S_1H(x) + S_2}{H(x) + 1}\theta(x) = K(x)\theta(x). \tag{22}$$

Therefore, the global torsional stiffness $K(x)$ of Eq. (6) is

$$K(x) = \frac{S_1H(x) + S_2}{H(x) + 1}. \tag{23}$$

Observe that Eq. (22) provides a relationship between the total twisting moment $M(x)$ and the total angular displacement $\theta(x)$, whereas the local torsional stiffness S_α in Eq. (16) relates the partial twisting moment $M_\alpha(x)$ with the partial torsional waves $\theta_\alpha(x)$. The local torsional stiffness S_α is a function of the material property only, while the global torsional stiffness $K(x)$ depends on the reflection coefficient R_1, and consequently on the boundary conditions.

4. NON-UNIFORM ROD SUBJECTED TO EXCITATION TORQUE

The torsional waves propagating in a non-uniform rod formed by uniform segments will be reflected and transmitted at the interfaces between the segments. Therefore, it is necessary to determine the expression for the reflection coefficient R of the interfaces.

Consider first the case of a rod composed of two parts, and subjected to a torque m at the interface ($x = L_1$) between the two segments, as shown in Fig. 3. It should be emphasized that if the torque is applied within a uniform segment, one must divide this segment to create an interface at the section where the torque is applied. From Eqs. (13a) and (22), one has for $x = L_1^-$

$$\theta(L_1^-) = \theta_1(L_1^-) + \theta_2(L_1^-) \tag{24a}$$

and

$$M(L_1^-) = K(L_1^-)\theta(L_1^-) - m. \tag{24b}$$

Now, writing Eqs. (17) and (18) for $x = L_1^+$ yields

$$M(L_1^+) = S_1\theta_1(L_1^+) + S_2\theta_2(L_1^+) \tag{25a}$$

and

$$\theta_1(L_1^+) = R_2\theta_2(L_1^+) + Qm. \tag{25b}$$

In Eqs. (25a) and (25b), R_2 is the coefficient of reflection at $x = L_1$ and Q is the term that transmits the effect of the external torque applied at $x = L_1$ to the other sections of the rod. Note that S_α, $\alpha = 1, 2$, in Eq. (25a), are the local torsional stiffness of segment 2. Substituting Eq. (25b) into Eqs. (13a) and (25a) yields:

$$\theta(L_1^+) = (1 + R_2)\theta_2(L_1^+) + Qm. \tag{26a}$$

and

$$M(L_1^+) = (S_1R_2 + S_2)\theta_2(L_1^+) + S_1Qm. \tag{26b}$$

The condition of continuity of angular displacement and twisting moment at $x = L_1$, $\theta(L_1^-) = \theta(L_1^+)$, and $M(L_1^-) = M(L_1^+)$, and substitution of Eq. (26a) into Eq. (24b) leads to

$$K(L_1^-)(I + R_2)\theta_2(L_1^+) + K(L_1^-)Qm - m = (S_1R_2 + S_2)\theta_2(L_1^+) + S_1Qm. \quad (27)$$

Therefore, from Eq. (27), one can conclude that the expressions for R_2 and Q are

$$R_2 = \frac{K(L_1^-) - S_2}{S_1 - K(L_1^-)} \quad (28a)$$

and

$$Q = \frac{1}{K(L_1^-) - S_1}. \quad (28b)$$

Repeating the same procedure presented in the preceding section to obtain Eq. (22), but now also employing Eqs. (25b) to (26b), that take into account the external torque applied to the rod, one can finally find

$$M(x) = K(x)\theta(x) + h(x)m; \quad (29)$$

where

$$h(x) = [S_1 - K(x)]W_1(x)Q \quad (30)$$

is the function that transfers to the other sections of the rod the effect of the moment m applied at $x = L_1$. The procedure described in this section will be used in the next section in a solution algorithm to obtain the torsional natural frequencies and distribution of angular displacement of stepped rods.

5. SOLUTION ALGORITHM FOR THE TORSIONAL VIBRATION OF STEPPED SHAFTS

The concepts presented in the preceding sections are now generalized to the case of non-uniform rods with arbitrary geometry, as illustrated in Fig. 4. Each uniform segment of the rod is labelled by an index $j = 1 \ldots N$. The interfaces between segments are also labelled by j, running from 1 to $N + 1$. It is assumed that the rod is connected at its left end to an element of known stiffness K_1. The stiffness of this element represents the boundary condition of the rod at $x = 0$. For example, if the rod is free one takes $K_1 = 0$; whereas, if its end is clamped one lets $1/K_1 = 0$. Non-classical boundary conditions can be implemented by using an appropriated value of K_1. Concentrated moments and concentrated elements such as rotary inertias and torsional springs applied along the rod can also be taken into account. For instance, consider a twisting moment m_1 at $x = 0$. The algorithm is composed of two parts, the first to determine the frequency response function and the second to obtain the distribution of angular displacement.

5.1. Frequency Response Function of the Rod

In the first part of the algorithm, the frequency response function of the rod is obtained as detailed below. Start from the left end of the rod, where the stiffness K_1 is known, then evaluate the stiffness K_2 at the second interface between segments 1 and 2 and so on until finally evaluating the stiffness

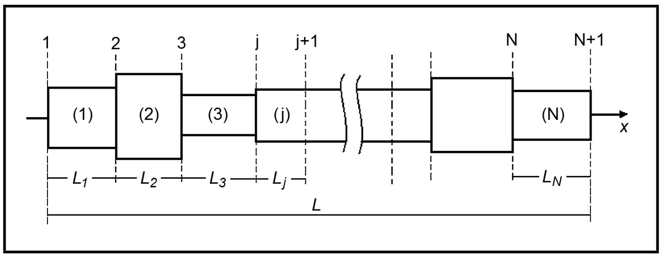

Figure 4. Shaft divided in N uniform segments.

K_{N+1} at the right end of the rod. The procedure is summarized in the following algorithm:

GIVEN ω, K_1 AND m_1 REPEAT FROM $j = 1$ TO N

$$\begin{aligned}
&R_j = \left(K_j - S_2^{(j)}\right) / \left(S_1^{(j)-K_j}\right);\\
&Q_j = 1/\left(K_j - S_1^{(j)}\right);\\
&H_j = W_1^{(j)}(L_j)R_j/\left(W_2^{(j)}(L_j)\right);\\
&h_j = \left(S_1^{(j)} - K_j\right)W_1^{(j)}(L_j)Q_j;\\
&K_{j+1} = \left(S_1^{(j)}H_j + S_2^{(j)}\right)/(H_j + 1);\\
&m_{j+1} = h_j m_j;
\end{aligned}$$

END.

Note that the superscripts (j) of S_α and W_α, $\alpha = 1, 2$, correspond to the segments of the rod, while the subscript j is used to designate the interfaces between the segments. To obtain, for example, the frequency response function of the angular displacement of the rod at $x = L$, one evaluates θ_{N+1} for each frequency ω using the algorithm and the following expression:

$$M_{N+1} = K_{N+1}\theta_{N+1} + m_{N+1}; \quad (31)$$

where M_{N+1} is the twisting moment at $x = L$. Also observe that m_{N+1} can also represent the contribution of the concentrated twisting moments applied along the rod to the angular displacement of the rod at $x = L$. The natural frequencies of the rod can be obtained from its frequency response or from the variation of the global torsional stiffness K_{N+1} in function of frequency.

5.2. Distribution of Angular Displacement

To evaluate the angular displacement along the rod, one has to march backwards using the following recursive algorithm:

REPEAT FROM $j = N$ TO 1

$$\begin{aligned}
&\theta_2^j = (1 + H_j)^{-1}\theta_{j+1} - (1 + H_j)^{-1}W_{1j}Q_jm_j;\\
&\theta_j = (I + R_j)W_{2j}^{-1}\theta_2^j + Q_jm_j;
\end{aligned}$$

END.

Note that the determination of the angular displacement distribution begins at $x = L$, where the angular displacement θ_{N+1} ($j = N$), determined using the first part of the algorithm and Eq. (31), is used to calculate the angular displacement θ_N at $x = L - L_N$. Then, proceed to θ_{N-1} at

$x = L - (L_{N-1} + L_N)$, and so on, until determining the angular displacement θ_1 at $x = 0$. It should be pointed out that each uniform segment of the rod can be arbitrarily subdivided into smaller segments to obtain a detailed description of a vibration mode. Note that one should record the values of H_j, Q_j, $W_{\alpha j}$, and m_j when performing the first part of the algorithm in order to use the recursive algorithm to determine the distribution of angular displacement.

6. EXAMPLE RESULTS

In this section the proposed method is demonstrated and the results are compared with the results obtained with other methods in the existing literature. Simulations using the commercial finite element (FEM) software COSMOS™/SolidWorks were also employed to verify the proposed method.

6.1. Uniform Rod with Concentrated Elements

The case of a uniform rod with concentrated elements was chosen to perform the first demonstration and verification of the proposed method. Natural frequencies obtained by Chen for a clamped free shaft with five rotary inertia using a numerical method that provides the exact solution for uniform circular shafts carrying multiple concentrated elements was used for comparison.[14] The problem is described as follows, using the nomenclature and units used by Chen[14] shown between parentheses: a circular shaft with length $L = 1016$ mm (40 in), diameter $d = 25.4$ mm (1.0 in), shear modulus of shaft material $G = 82.74 \times 10^9$ Pa (1.2×10^7 psi), mass density of shaft material $\rho = 7,839$ kg/m^3 (0.283 lbm/in^3), with five non-dimensional concentrated rotary inertias given by $I^*_{0v} = \overline{J}_p L / I_{0v}$, where $\overline{J}_p$ is the mass moment of inertia about the rotational axis (x) per unit length and I_{0v} represents the vth attached rotary inertia. The locations of the rotary inertias are: $\xi_1 = 0.1$, $\xi_2 = 0.3$, $\xi_3 = 0.5$, $\xi_4 = 0.7$, and $\xi_5 = 0.9$, where $\xi_j = x_j/L$, $j = 1$ to 5. To determine the natural frequencies using the method proposed here, one should use the algorithm presented in subsection 5.1.

Starting from the clamped end, a large value to the stiffness K_1 should be taken to represent this boundary condition. If one is interested only in the natural frequencies, a unique segment is necessary for each uniform part of the shaft; otherwise, if the distribution of angular displacement must also be known, the uniform parts of the shaft should be subdivided arbitrarily in smaller segments. In this problem the concentrated rotary inertia was represented by a thin large diameter disc. The diameters are determined according to the values of the rotary inertias. A comparison between the results obtained by Chen[14] and the corresponding ones obtained using the proposed algorithm is presented in Table 1 for the lowest five natural torsional frequencies. As the length of the rotary inertia is reduced, the values of the natural frequencies converge to the results obtained by Chen.[14] An almost perfect agreement of results is observed in Table 1 using disks with 0.005 in length with large diameters as concentrated rotary inertias. Nevertheless, it should be emphasized that the method does not account for the Poisson's effect or for any cross-section deformation, and therefore cannot model accurately the high frequency vibration.

Table 1. Comparison with the results obtained by Chen[14] for the lowest five natural torsional frequencies of the clamped-free shaft carrying five rotary inertia.

Method	Torsional Natural Frequencies (rad/s)				
	ω_1	ω_2	ω_3	ω_4	ω_5
Chen[14]	104.09671	304.98929	482.88004	619.40419	694.81096
Proposed Method	104.10	305.09	483.06	619.65	695.16

Table 2. Comparison between the lowest five torsional natural frequencies obtained with the proposed method and the FEM for a stepped shaft with five segments.

B.C.	Method	Torsional Natural Frequencies (rad/s)				
		ω_1	ω_2	ω_3	ω_4	ω_5
C-F	Proposed Method	9432	54823	74995	111400	140890
	FEM	9356	53956	73739	110070	139630
	Difference (%)	0.81	1.61	1.70	1.21	0.90
F-F	Proposed Method	41023	65849	90354	123760	152650
	FEM	40188	64610	88530	122500	150320
	Difference (%)	2.08	1.92	2.06	1.03	1.55

6.2. Stepped Shaft

The proposed method will now be evaluated through comparisons with the FEM results. First, to check the finite element model and analysis, the exact values of natural frequencies of a uniform shaft were calculated and compared to FEM results. In the following FEM analysis, we have adopted tetrahedral mesh model. The mesh was refined around geometrical details. Convergence tests have been performed to ensure the calculated natural frequencies.

FEM results obtained for the torsional vibration of an arbitrary stepped shaft composed of five segments with lengths equal to $L_1 = 60$, $L_2 = L_3 = 50$, $L_4 = 80$, and $L_5 = 70$ mm and diameters $D_1 = 30$, $D_2 = 35$, $D_3 = 40$, $D_4 = 50$, and $D_5 = 40$ mm, shear modulus $G = 77$ GPa, and mass density $\rho = 7900$ kg/m^3, are compared to the results obtained with the proposed method. The lowest five natural frequencies for the free-free (F-F) and clamped-free (C-F) boundary conditions (B.C.) are presented in Table 2. The natural frequencies were obtained using the algorithm presented in subsection 5.1. The FEM analysis was implemented using solid elements and a modal shape analysis.

Table 2 also shows the difference between the values of the torsional natural frequencies obtained by the proposed method and the FEM. One can note that the results are in good agreement, with a maximum difference of approximately 2%.

6.3. Rod with a Continuously Varying Geometry

In this section, the proposed method is evaluated, as well as an approximated solution for the torsional vibration of rods with continuously varying geometry. Consider a rod with continuously-varying diameter, as for example a conical rod. To address this problem, a stepped cone, i.e., a cone composed of uniform segments with different diameters, is used as an approximation to the conical rod. In order to verify the accuracy of the method for determining the torsional natural frequencies of continuously varying systems, the natural frequencies of truncated cones (Fig. 5) with different angles, shear modulus

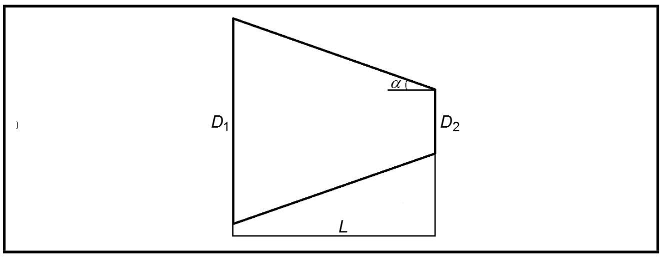

Figure 5. Truncated cone.

$G = 77$ GPa, and mass density $\rho = 7900$ kg/m^3 were determined and compared to the corresponding ones obtained using the FEM. The diameter $D_1 = 60$ mm and the cone length $L = 30$ mm were kept constant while the angle α was increased from $\alpha = 5°$ to $\alpha = 30°$ in order to obtain different values of $\Delta = 1 - D_2/D_1$.

The lowest two torsional natural frequencies for a clamped-free boundary condition were determined for each cone using an increasing number of segments until the value of each natural frequency converged. The segments of the stepped rod had the same length (L/N) and the diameter of each segment was equal to the diameter of the mid-segment. Table 3 presents a comparison between the results obtained using commercial finite element software and the method proposed in this paper. Solid elements were employed to model the cone. A modal shape analysis was performed and the values of torsional natural frequencies were identified among the results provided by the FEM. As expected, a good agreement between the results was observed for small values of Δ; i.e., the accuracy of the proposed method decreases if the rod geometry becomes very different from a cylindrical rod. Even if the number of segments are increased, the proposed method cannot provide a good accuracy for large values of Δ.

6.4. Shaft with Uniform Parts and a Conical Segment

A shaft with a geometry composed of two uniform parts and a conical section, as depicted in Fig. 6, with shear modulus $G = 77$ GPa and mass density $\rho = 7900$ kg/m^3, was also analysed using the proposed method. A comparison between the lowest two torsional natural frequencies for a free-free and clamped-free boundary condition obtained with the FEM and the proposed method are shown in Table 4. Figure 7 presents a comparison between the angular displacements along the shaft determined using the method presented in this work and the FEM. According to Table 4 and Figs. 7(a) to 7(d), the results obtained by the proposed method and the FEM are in good agreement. To determine the distribution of angular displacement, the uniform parts of the rod can be subdivided into any number of smaller segments. The distribution of angular displacement is obtained using the second part of the solution algorithm described in section 5. The rod should be subdivided into smaller segments, as short as necessary, to obtain the complete description of a vibration mode. A stepped cone was used as an approximation to the conical part of the shaft. In this example, the uniform parts and the conical part were subdivided into segments of 1.0 mm length ($N = 500$).

Table 4. Lowest two torsional natural frequencies (rad/s) for the shaft shown in Fig. 6.

Boundary Condition	Method	ω_1	ω_2
Free-free	FEM	25445	38184
	Proposed Method	25950	37910
	Difference (%)	1.9	0.7
Clamped-free	FEM	15093	26178
	Proposed Method	14990	27010
	Difference (%)	0.7	3.1

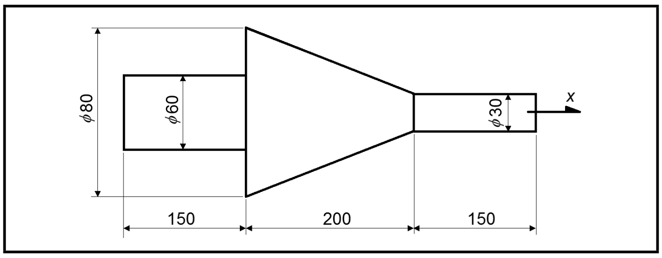

Figure 6. Shaft with a conical part and uniform segments (dimensions in millimetres).

7. CONCLUSIONS

A new method to study the torsional vibration of non-uniform rods has been developed using a theory usually applied to investigate the wave propagation in layered media. A simple and efficient algorithm based on the discrete form of the Riccati transformation has been proposed to determine the torsional natural frequencies and angular displacement distribution of stepped shafts. The algorithm is computationally efficient and very easy to implement. The proposed method was evaluated through comparisons with analytical and finite element method. The results show that the proposed solution algorithm may provide exact results for uniform shafts with concentrated elements and accurate results for stepped shafts. Systems with continuously varying geometry can be properly represented by stepped geometries; however, the accuracy of the method decreases if the continuous system becomes very different from a uniform rod.

REFERENCES

1. Chin, R. C. Y., Hedstorm, G. W., and Thigpen, L. Matrix methods in synthetic seismograms, *Geophysical Journal of the Royal Astronomical Society*, **77** (2), 483–502, (1984).

2. Keller, H. B. and Lentine, M. Invariant imbedding, the box scheme and an equivalence between them, *SIAM Journal on Numerical Analysis*, **19** (5), 942–962, (1982).

3. Dieci, L., Osborne, M. R., and Russel, R. D. A Riccati transformation method for solving linear BVPs. I: theoretical aspects, *SIAM Journal on Numerical Analysis*, **25** (5), 1055–1073, (1988).

4. Dieci, L., Osborne, M. R., and Russel, R. D. A Riccati transformation method for solving linear BVPs. II: computational aspects, *SIAM Journal on Numerical Analysis*, **25** (5), 1074–1092, (1988).

5. Braga, A. M. B., Honein, B., Barbone, P. E., and Herrmann, G. Suppression of Sound Reflected from a Piezoelectric Plate, *Journal of Intelligent Material Systems and Structures*, **3** (2), 209–223, (1992).

Table 3. Lowest two torsional natural frequencies (rad/s) for truncated cones with different $\Delta = 1 - D_2/D_1$ ($\alpha = 5°$, $10°$, $20°$ and $30°$).

Method	$\Delta = 0.087$ $(\alpha = 5°)$		$\Delta = 0.19$ $(\alpha = 10°)$		$\Delta = 0.364$ $(\alpha = 20°)$		$\Delta = 0.577$ $(\alpha = 30°)$	
	ω_1	ω_2	ω_1	ω_2	ω_1	ω_2	ω_1	ω_2
Proposed Method	175800	494780	190038	500484	287115	558220	287115	558220
FEM	175740	492480	188800	494500	220260	499870	265800	514540
Difference (%)	0.03	0.5	0.8	1.2	3.3	3.8	8.0	8.5

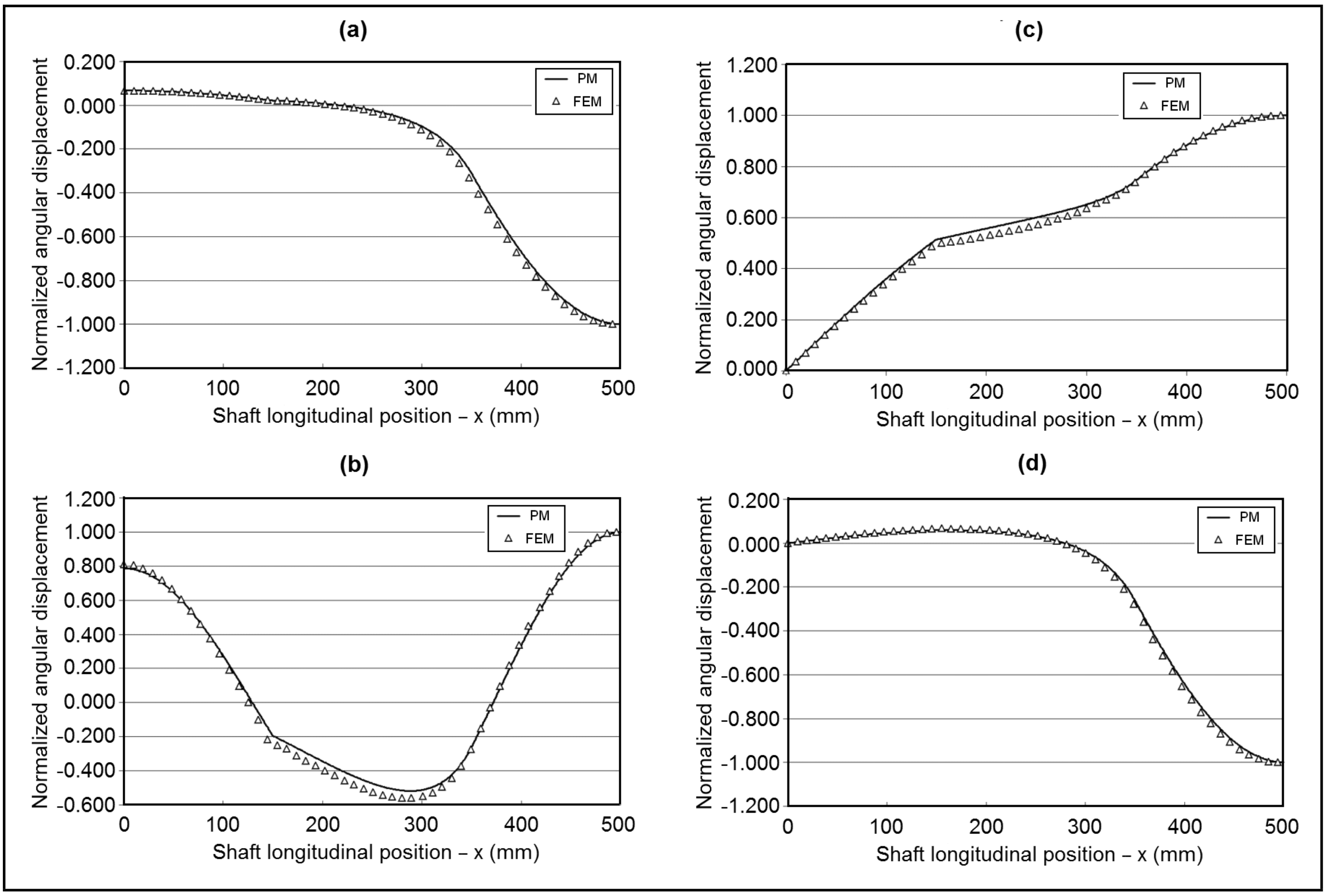

Figure 7. Comparison between the distribution of angular displacement obtained by the proposed method (PM) and the FEM of the shaft described in Fig. 6 for different boundary conditions: (a) and (b) first and second vibration modes free-free, (c) and (d) first and second vibration modes clamped-free, respectively.

[6] Braga, A. M. B., de Barros, L. P. F., and Gama, A. L. Models for the high frequency response of active piezoelectric composite beams, *Smart Materials and Structures, Proceedings of the 4th European and 2nd MIMR Conference*, 115–122, (1998).

[7] Langley, R. S. Wave evolution, reflection, and transmission along inhomogeneous waveguides, *Journal of Sound and Vibration*, **227** (1), 131–158, (1999).

[8] Lee, S. K., Mace, B. R., and Brennan, M. J. Wave propagation, reflection and transmission in non-uniform one-dimensional waveguides, *Journal of Sound and Vibration*, **304** (1–2), 31–49, (2007).

[9] Pouyet, J. M. and Lataillade, J. L. Torsional vibrations of a shaft with non-uniform cross section, *Journal of Sound and Vibration*, **76** (1), 13–22, (1981).

[10] Qiao, H., Li, Q. S., and Li, G. Q. Torsional vibration of non-uniform shafts carrying an arbitrary number of rigid disks, *Journal of Vibration and Acoustics*, **124** (4), 656–659, (2002).

[11] Li, Q. S. Torsional vibration of multi-step non-uniform rods with various concentrated elements, *Journal of Sound and Vibration*, **260** (4), 637–651, (2003).

[12] Mioduchowski, A. Torsional waves and free vibrations of drive systems with stepped shafts, *Archive of Applied Mechanics (Ingenieur Archiv)*, **56** (4), 314–320, (1986).

[13] Bapat, C. N., and Bhutani, N. General approach for free and forced vibrations of stepped systems governed by the one-dimensional wave equation with non-classical boundary conditions, *Journal of Sound and Vibration*, **172** (1), 1–22, (1994).

[14] Chen, D.-W. An exact solution for free torsional vibration of a uniform circular shaft carrying multiple concentrated elements, *Journal of Sound and Vibration*, **291** (3–5), 627–643, (2006).

[15] Xiang, L., Yang, S., and Gan, C. Torsional vibration measurements on rotating shaft system using laser Doppler vibrometer, *Optics and Lasers in Engineering*, **50**, 1596–1601, (2012).